Experimental Investigation on Corrosion Behavior of Ultrasonic Assisted stir Cast AA6061 Hybrid Metal Matrix Composite under DifferentAqueous Corrosive Environments

Rajakumar Murugan[a]* , Prince Sahaya Sudherson Deva sahayam[a], Ashok raj Rajendran[b] ,

Bensam Raj Jesuretnam[c]

[a]Rohini college of Engineering and Technology, Department of Mechanical Engineering, 629401, Kanyakumari, Tamil Nadu, India.
[b]J.J College of Engineering and Technology, Department of Mechanical Engineering, 620009, Trichy, Tamil Nadu, India.
[c]Muthayammal Engineering College, Department of Mechanical Engineering, 637408 Namakkal, Tamil Nadu, India.

Aluminum Hybrid Metal Matrix Composites (Al-HMMCs) are contemporary materials that blend aluminum with additional reinforcing elements to enhance their mechanical, thermal, and other properties. These materials find applications across various sectors including the aerospace industry, automotive sector, military and defence, marine industry, as well as manufacturing industries. In this research, AA6061, zirconium dioxide (ZrO_2) and boron carbide (B_4C) have been selected as the matrix and reinforcement materials. AA6061/ZrO_2/B_4C (Al-HMMCs) is manufactured using Ultrasonic-assisted stir casting. The process parameters of ultrasonic assisted stir casting were optimized with the help of Taguchi optimization technique. The melting temperature (700, 750 and 800 ºC), stirring speed (10, 15 and 20 minutes) and AA6061/xwt.%B_4C/xwt.%ZrO_2 (6, 8 and 10) are selected as input parameters for optimization. The reinforcements ZrO_2 and B_4C are weighed by equally sharing by wt.% The micro hardness was selected as response parameter and it was determined by using Vickers micro hardness tester. The L9 Orthogonal Array (OA) was employed for optimization of input parameters of ultrasonic assisted stir casting. Taguchi results showed that medium level of melting temperature (750 ºC), higher level of stirring speed (300 rpm), lower level of stirring duration (10 minutes) and medium level of wt.% of ZrO_2 and B_4C (8wt.%) were the optimized combination of input process parameters of ultrasonic assisted stir casting for fabricating AA6061 HMMC. The AA6061/xwt.%B_4C/xwt.%ZrO_2 (x = 0,4,6,8 and 10) HMMCs were manufactured by utilizing optimized process parameters. The micro hardness of AA6061/xwt.%B_4C/xwt.%ZrO_2 (x = 0,4,6,8 and 10) was determined. . From the obtained hardness tests, it was observed that the hardness of AA6061 HMMCs was enhanced up to addition of 8wt. % of B_4C and ZrO_2 and decreased the hardness while adding 10wt.% of B4C and ZrO_2. The better AA6061/8wt.%ZrO_2/8wt.%B_4C HMMC undergone X-ray Diffraction Analysis (XRD) and Scanning Electron Microscope (SEM) testing to identify elements and examine the microstructure. The high peak of ZrO_2, B_4C and Al was obtained in 71.4, 35.68 and 37.81 2 theta values respectively. The SEM image of ultrasonic aided stir cast AA6061 based composite was confirmed the uniform distribution of zirconium di oxide and boron carbide reinforcements. There was no oxide formation on the surface of the stir casted AA6061 composites due to the execution of casting process in the inert environment. The casted AA6061/8wt.%ZrO_2/8wt.%B_4C surface of the composite exhibits no porosity occurrence due to the impact of usage of ultrasonic vibrator to prevent the formation of holes due to escape of unwanted gases. Subsequently, corrosion tests were conducted on the AA6061 HMMC in various corrosive environments such as NaOH, HCl, H_2SO_4, and NaCl to evaluate its electrochemical behavior. The surfaces of corroded specimens were analyzed using SEM and Energy Dispersive Spectroscopy (EDS). The research findings indicate that AA6061 composites exhibit the highest corrosion resistance when immersed in a NaCl medium. This enhanced resistance was attributed to the medium's lower corrosion potential, stronger charge transfer resistance (Rct), and lower double-layer capacitance (Cdl) compared to alternative environments. Additionally, SEM analysis illustrated that the incorporation of B_4C and ZrO_2 ceramics results in the formation of protective barrier layers, further enhanced their corrosion resistance. ZrO_2 particles were attracted and neutralized the corrosive ions and electrons, thereby reducing corrosive activity on the AA6061 aluminium matrix.

Keywords: *AA6061, ZrO2, B4C, Corrosion resistance, XRD, EDS, SEM.*

*e-mail: rajakumar1947@gmail.com

1. Introduction

Countless scientific research discoveries contribute to the continual advancements in sophisticated engineering materials utilized across automotive, marine, aviation and building construction industries[1,2]. Advanced engineering materials encompass composite materials, which are classified based on their matrix[3]. Among these materials, metal matrix composites (MMCs) represent one type. Various metals, including titanium, magnesium, and aluminum, have served as base matrices. However, the aluminum matrix has been the primary focus of study[4-6]. Aluminum matrix composites (AMCs) represent versatile materials employed across various fields of mechanical engineering. Recently, they have garnered significant attention owing to their combination of high specific strength, low thickness, superior quality, favourable weight-to-strength ratio, and relatively high wear resistance[7-9]. The exceptional physico-mechanical characteristics of AMCs have led to their utilization in the automotive and aviation industries[10]. These composites are produced by incorporating numerous monolithic and hybrid reinforcements into aluminum matrices[11]. Both natural and synthetic materials such as SiC, Al_2O_3, B_4C, and TiC serve as reinforcements[12]. Several manufacturing techniques can be employed for the creation of MMCs, including powder metallurgy, high-energy ball milling, stir casting, spray deposition, and squeeze casting[13]. However, stir casting is predominantly favoured due to its simplicity, cost-effectiveness, and ability to achieve a uniform dispersion of reinforcing particles throughout the matrix[14]. The presence of pores in the casting diminishes the material's strength, with hydrogen trapped in the molten metal being the primary cause. Ultrasonically aided stir casting, which eliminates the need for degassing and is renowned for its affordability and environmentally friendly approach, is a commonly adopted technique to mitigate this issue and produce flawless castings[15]. While adding reinforcements can enhance the physico-mechanical features of MMCs, it is essential to recognize that this can also significantly influence their corrosion resistance. When assessing the application potential of AMCs, one of the most critical factors to consider is their corrosion behavior[16]. Using the stir casting technique, the effects of adding graphite, Al_2O_3, SiC, and B_4C reinforcements at 4% and 5% were investigated. The resulting specimens were immersed in solutions containing 3.5% NaCl and 1M HCl, followed by thorough evaluations. The findings revealed good mechanical properties and notable corrosion resistance. Furthermore, the impact of adding hybrid RHA and Al_2O_3 particles in similar quantities (1–5 wt%) to A356 alloy under various aging conditions was examined. The stir casting process was employed to fabricate the specimens, which were then submerged in 5% and 0.1 normal HCl solutions. The investigation demonstrated an enhancement in the corrosion resistance of composite[17]. ZrO_2 stands out as a highly desirable reinforcing material due to its density of 8.18 g/cm³, melting temperature of 1860°C, UTS of 425 MPa, VHN of 150, and Young's modulus of 98 GPa. Additionally, it has been observed that ZrO_2 demonstrates enhanced strength, hardness, and fracture toughness, with only a slight decrease in ductility[18]. Utilizing PDP and EIS to analyze the corrosion behavior of Al/B_4C AMCs in four distinct environments, it was determined that their charge transfer resistance exceeded that of the matrix

alloy by approximately 23-59%. Moreover, their corrosion rate was significantly reduced, with decreases of 22-42% in NaOH and nearly 99% in the NaCl medium[19]. Stir casting was employed to fabricate AA 6061 alloy composites reinforced with ilmenite (FeTiO3) particles at various weight percentages (5%, 10%, and 15%). This study investigated the hardness, wear resistance, coefficient of friction, and pitting corrosion behavior of the resulting composites. The findings indicated that the incorporation of ilmenite as reinforcement increased the hardness of the AA 6061 alloy while decreasing the wear rate and coefficient of friction. Particularly, the 10% ilmenite composite exhibited superior resistance to pitting corrosion compared to other composites and the base metal[20]. Within the given input parameters, the most impactful factors are the stirring speed set at 600 revolutions per minute, ultrasonic vibration for 2 minutes, and an ultrasonic vibration depth of 40 millimeters. The resulting data from these conditions include a porosity level of 1.4%, an ultimate tensile strength of 247 MPa, and a wear rate measured at 0.0013 mm³ per minute[21]. The findings indicated that setting the process parameters to a stirrer speed of 400 revolutions per minute, an ultrasonic power of 1500 watts, and a 3 wt% concentration of TiB_2 reinforcement achieved the highest grey relational grade. This optimal combination led to the creation of a composite material characterized by superior microhardness and reduced wears[22]. The Aluminum Metal Matrix Nano Composites (AMMNCs) exhibited distinct phases due to the even dispersion of nano-ZrB_2 particles, as confirmed by X-ray diffraction testing and microstructural analysis at the micron level. The addition of ZrB_2 reinforcements resulted in increased toughness of the composite materials, and at a 2 weight percent of reinforcement, the wear rate decreased. Moreover, it was observed that the corrosion potential shifted from -684 to -462 mV during static immersion corrosion testing of AMMNCs in a 3.5 weight percent NaCl aqueous solution, leading to a reduction in corrosion current density[23]. The extent of corrosion and the size of corrosion pits were found to be greater under UV light exposure compared to dark conditions. This phenomenon was attributed to the increased dissolution of AlFeSi intermetallics and fewer oxides, such as Al_2O_3, forming when exposed to UV radiation. After a 4-week exposure period, it was noted that passive film formation exhibited fewer defects under UV radiation, resulting in more compact structures that enhanced the protection of the aluminium substrates and consequently inhibited corrosion to a certain extent[24]. After reviewing the work of numerous early researchers, it is evident that there has been no investigation conducted on the corrosion behavior of AA6061/ZrO_2/B4C composites under various corrosive environments. This current study explores the electrochemical corrosion behaviour of ultrasonically assisted stir cast AA6061/B_4C/ ZrO_2 under different aqueous corrosive environments, including NaOH, HCl, H_2SO_4, and NaCl. Achieving a uniform distribution of B_4C particles in the AA6061 matrix is challenging. Poor wettability leads to weak interfacial bonding between the matrix and reinforcement particles, which negatively affect the overall strength and durability of composites. B_4C particles have a tendency to cluster together, forming agglomerates that weaken the mechanical properties of composite materials. Stir casting often introduces gas bubbles into the melt, which can become

Experimental Investigation on Corrosion Behavior of Ultrasonic Assisted stir Cast AA6061 Hybrid Metal
Matrix Composite under DifferentAqueous Corrosive Environments

3

Table 1. Elements of AA6061.

Element	Si	Mg	Cu	Fe	Mn	Cr	Zn	Ti	Al
Wt.%	0.6	1	0.27	0.34	0.14	0.04	0.24	0.14	Bal.

trapped and form porosity within the composite. ZrO_2 improves the wettability of B_4C with the aluminium 6061 matrix by providing a more favourable surface energy for bonding and by promoting better interfacial reactions. ZrO_2 aids in preventing agglomeration of B_4C particles by acting as a spacer and promoting uniform dispersion, leading to a more homogenous composite structure. The addition of ZrO_2 to B_4C in AA6061 matrix composites helps to address the challenges of poor wettability and agglomeration associated with B_4C alone. ZrO_2 improves the wetting behavior of the matrix with B_4C, facilitating better bonding and integration. It also aids in dispersing B_4C particles more uniformly, reducing agglomeration and leading to a composite with superior mechanical ,physical and corrosion properties. Incorporating B_4C and ZrO_2 into an AA6061 aluminum matrix using stir casting methods presents several challenges related to wettability, particle dispersion, reactive nature, processing complexity and control over particle size. The challenges can overcome by using ultrasonic assisted stir casting method. Ultrasonic-assisted stir casting method is particularly advantageous when incorporating B_4C reinforcements into AA6061 aluminum matrix material. It addresses challenges related to particle dispersion, porosity reduction, interface bonding, microstructural control, and process efficiency.

2. Materials and Methods

2.1. Materials

AA6061 alloy has moderate strength properties suitable for general applications, but it may not meet the high-strength requirements of demanding applications such as aerospace or automotive industries. It exhibits moderate hardness, which may limit its wear resistance in abrasive environments. Its inherent hardness may not be sufficient to resist wear compared to composite materials with reinforced phases like ceramics or fibers. While AA6061 has good corrosion resistance in atmospheric conditions and mild environments, it may not offer sufficient protection against corrosive substances or aggressive chemicals encountered in industrial settings. However, its corrosion resistance and wear resistance are moderate, necessitating the enhancement of its corrosion and tribological properties[25]. The moderate hardness, medium strength and corrosion resistance of AA6061 under aggressive chemical environments can be enhanced by adding boron carbide and zirconium di oxide into AA6061 matrix alloy. Hence the boron carbide and zirconium di oxide are selected as reinforcements to form AA6061 HMMCs. B_4C has a low density (2.52 g/cm^3), which is advantageous for applications requiring high strength-to-weight ratios, such as in aerospace and automotive industries. The strategic use of B_4C to significantly boost the hardness of composite while maintaining a lightweight structure is innovative. ZrO_2 has excellent chemical stability and resistance to oxidation and corrosion.

Table 2. Elements of ZrO_2 and B_4C.

Element	Zr	O	B	C
Wt.%	34.12	65.88	71.7	28.3

Zirconium dioxide and boron carbide exhibit superior corrosion resistance and wear resistance properties. Consequently, AA6061 and ZrO_2 with B_4C were chosen as the matrix and reinforcements, respectively. The AA6061 was procured in cylindrical form from Trichy Metal Alloys, located in Trichy, Tamil Nadu, India. The reinforcements, ZrO_2 and B_4C, were obtained as powder particles with an average size of 10 and 2 µm respectively from Sigma Aldrich with the assistance of Subra Scientific Company. The elements present in the AA6061 matrix and ZrO_2 with B_4C are listed in Table 1 and Table 2. The microstructure of ZrO_2 and B_4C is depicted in Figure 1.
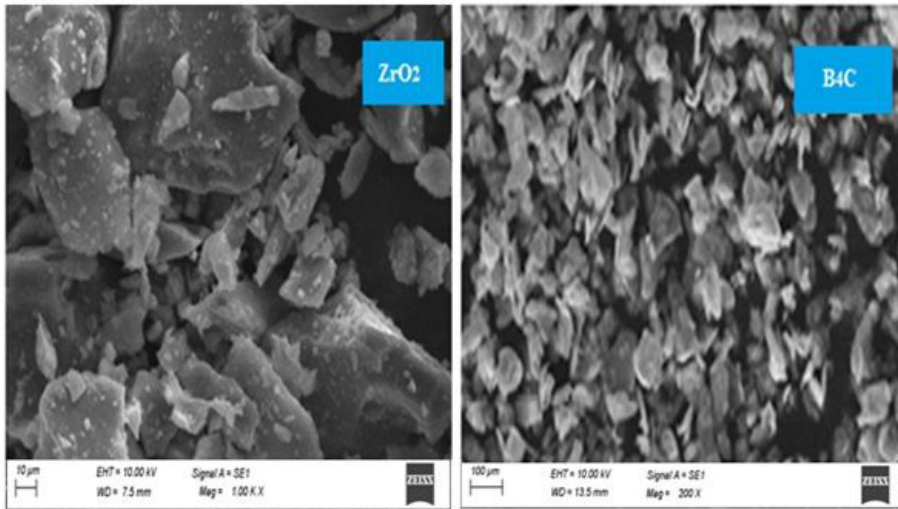
2.2. Fabrication of composite

The ultrasonic assisted stir casting was employed to manufacture the AA6061 HMMCs. The process parameters of ultrasonic assisted stir casting were optimized with the help of Taguchi optimization technique. The melting temperature (700, 750 and 800 ºC), stirring speed (10, 15 and 20 minutes) and AA6061/xwt.%B_4C/xwt.%ZrO_2 (6, 8 and 10) were selected as input parameters for optimization. The cylindrical AA6061 rod was cut into smaller pieces to facilitate placement of the matrix material in the electric furnace. The reinforcements ZrO_2 and B_4C were weighed by equally sharing by wt.% with the help of electronic weighing machine with an accuracy of 0.001 g. The weighed ZrO_2 and B_4C reinforcements were preheated at the temperature of 300 ºC for 2 hours to remove the volatile contaminants and moisture with the help of Muffle furnace. The preheated reinforcements were introduced into the molten AA6061 matrix. The probe of the ultrasonic sonicator was submerged in a mixture of molten materials, causing the molten material to vibrate at a high frequency of 20 kHz[7,26,27].

By using the high-frequency energy present in the molten material, this cavitations effect helped to ensure that the reinforcing particles were distributed evenly. The melt was done in inert environment to prevent oxidation. Employing the ultrasonic-assisted stir casting process, molten Al6061 containing a ZrO_2/B_4C reinforcing combination is introduced into the die. The die is heated to 450°C to counteract any potential shrinkage effects. The micro hardness was selected as response parameter. The L9 was employed for optimization of input parameters of ultrasonic assisted stir casting. The same procedure was followed to fabricate AA6061 HMMCs as per L9 OA. Table 3 shows the L9 Orthogonal Array with input and response parameters. The AA6061/xwt.%B_4C/xwt.%ZrO_2 (2,4,6,8and 10) were manufactured by using optimized process parameters of ultrasonic assisted stir casting. The ultrasonic stir casting setup and process flow for casting are displayed in Figure 2 and Figure 3.

Table 3. L9 with input and response parameters.

Ex.No	Melting temperature ºC	Stirring speed rpm	Stirring duration minutes	wt.% of B_4C and ZrO_2
1	700	200	10	6
2	700	250	15	8
3	700	300	20	10
4	750	200	15	10
5	750	250	20	6
6	750	300	10	8
7	800	200	20	8
8	800	250	10	10
9	800	300	15	6

Figure 1. SEM image of reinforcements.

Figure 2. Ultrasonic assisted stir casting setup.

Experimental Investigation on Corrosion Behavior of Ultrasonic Assisted stir Cast AA6061 Hybrid Metal
Matrix Composite under DifferentAqueous Corrosive Environments
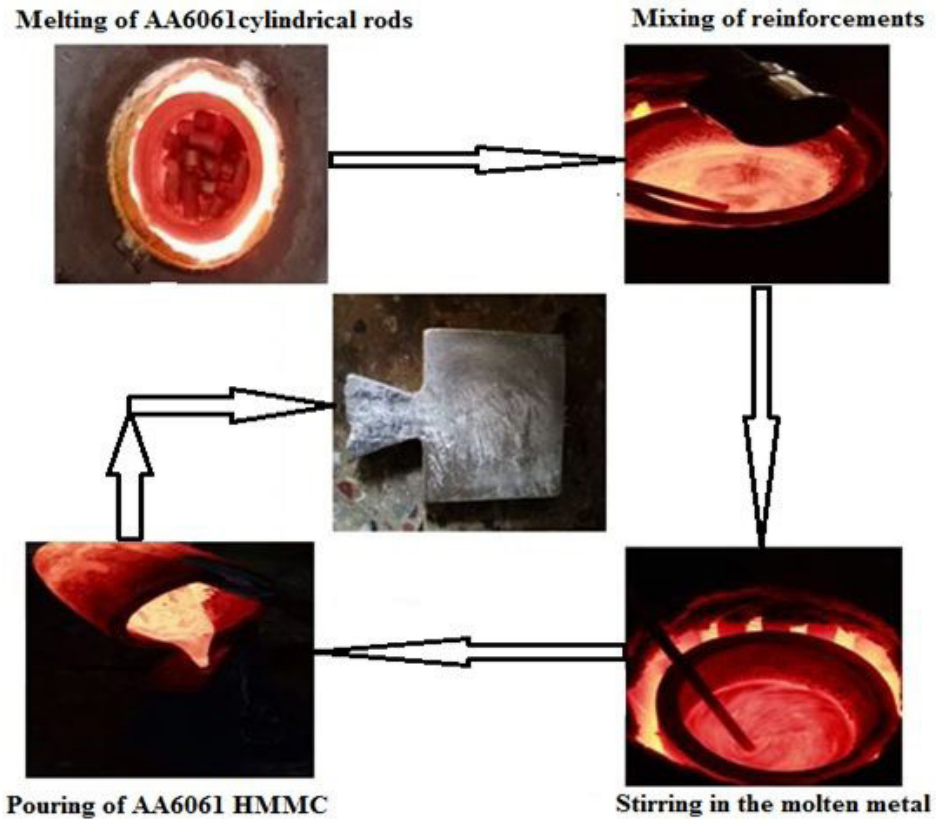
5

Figure 3. Casting process flow of AA6061 HMMCs.

2.3. Testing on composites

The manufactured AA6061/xwt.%B_4C/xwt.%ZrO_2 (2, 4, 6, 8 and 10) HMMCs were subjected to micro hardness testing. Wire-cut EDM (Princiwire) was utilized to cut the manufactured AA6061 HMMC to the required ASTM size for various tests without causing dislocation of atoms during cutting, thereby ensuring that the properties of the composites remained unchanged[28]. The microhardness test was conducted on the AA6061-based composite according to ASTM E384 standards, with a 350 g applied load for duration of 15 seconds, using a Micro hardness tester (HVD-1000 MT/HVD-1000AT). Three trials were conducted, and the average microhardness value was recorded. The better combination of AA6061 HMMC was selected based on microhardness test results for further investigation. The ultrasonically assisted stir-cast better combination of AA6061/ZrO_2/B_4C HMMC underwent XRD and SEM testing to confirm the presence of the matrix and reinforcements, as well as to verify the uniform dispersion of both ZrO_2 and B_4C in the AA6061 matrix. The surface of the AA6061 HMMC was polished using different abrasive grade sheets such as 600, 800, 1000, and 1200[29]. The surface of the AA6061 HMMC was polished to achieve a roughness of 1 μm, as confirmed by a surface roughness tester (MICROSURF 10). XRD testing on the AA6061 HMMC was conducted following ASTM E1123-86 standards using XtaLAB mini II . SEM testing on the AA6061-based composite was performed according to ASTM E1508-08 using CIQTEK 3200[30].

The experimental densities of the better combination of AA6061 HMMC and the matrix alloy were determined using the Archimedes principle, employing an analytical balance (Shimadzu-AUX-220, SMK-401).

AA6061 components used in marine applications, such as boat hulls, offshore structures, and marine equipment, are exposed to saltwater containing NaCl. Sulphuric acid is used in battery electrolytes and production processes. AA6061 components in battery casings or terminals may encounter H_2SO_4 exposure. AA6061 parts used in metal finishing processes, where HCl is employed for surface preparation or cleaning before plating or coating.AA6061 components used in chemical processing equipment may come into contact with NaOH solutions during cleaning, neutralization, or manufacturing processes. Many environments involve exposure to acidic substances. HCl is a strong acid and commonly found in various industrial processes. Testing in HCl helps evaluate the material's durability and resistance to acidic corrosion, which is crucial for applications in acidic environments. Many industrial applications involve handling sulfuric acid or acidic solutions. Testing under H_2SO_4 simulates these conditions, ensuring that AA6061 HMMCs meet performance requirements in acidic environments encountered in industries such as chemical processing, mining, and automotive. This testing is essential for industries requiring materials with robust resistance to acidic corrosion, ensuring long-term performance and operational safety[31].

Hence, corrosion tests were carried out in various corrosive environments, including H_2SO_4, NaOH, NaCl, and HCl. These chemicals were obtained from Sigma Aldrich with the assistance of Subra Scientific Company, Bangalore, India, with a purity exceeding 99.6%. The details of the corrosive media are presented in Table 4. ASTM G61 standards were followed for conducting corrosion tests on better combination of AA6061/ZrO$_2$/B$_4$C HMMC[32]. The Autolab PGSTAT 302N instrument and a three-electrode cell were used for corrosion measurements. In this setup, the sample served as the anode, while platinum wire (Pt) and an Ag/AgCl (3 M KCl) reference electrode were used as electrodes.

The samples underwent metallographic polishing to expose a 1.0 cm^2 region to the corrosive environment prior to the experiments. The open-circuit potential (OCP) was monitored for 1 hour to establish a stable potential range for the samples in different electrolytes. Potentiodynamic polarization (PDP) plots were generated within a voltage range of -0.2 V to -1.8 V vs. OCP, using a scanning rate of 0.1 mV/s. Electrochemical impedance spectroscopy (EIS) tests were conducted by applying a 5 mV AC voltage across a frequency range spanning from 10 Hz to 10,000 kHz.

The examination of the morphology for both the as-prepared and corroded samples of better combination of AA6061/ZrO$_2$/B$_4$C-based composites (HMMC) was performed. The samples were embedded in epoxy resin and polished using SiC papers up to a 2000-grit finish, followed by cleaning with ethanol, acetone, and deionized water. Surface morphology was then observed using Keller's reagents (a solution containing 95 mL of water, 1.0 mL of HF, 2.5 mL of HNO$_3$, and 1.5 mL of HCl)[33]. Scanning electron microscopy (SEM) coupled with energy-dispersive X-ray spectroscopy (EDS) was employed to investigate the AA6061/ZrO$_2$/B$_4$C.

3. Results and Discussion

3.1. Optimization of ultrasonic assisted stir casting process parameters of AA6061 HMMC

The Mini tab 19 software is used for optimizing the process parameters according to Taguchi technique with the higher the better choice. Table 5. shows the L9 Orthogonal Array with input and response parameters.

Response Table 6 shows that medium level of melting temperature (750 ºC), higher level of stirring speed (300 rpm), lower level of stirring duration (10 minutes) and medium level of wt.% of ZrO$_2$ and B$_4$C (8wt.%) are the optimized combination of input process parameters of ultrasonic assisted stir casting for fabricating AA6061 HMMC. The main effect plot for Vickers hardness is displayed in Figure 4.

The confirmation test is done on the AA6061 HMMC, which is manufactured by the optimized process parameters of ultrasonic assisted stir casting process. Three trails are

Table 4. Details of corrosive mediums.

S.No	Corrosive environments	Medium	PH	Molarity
1	Acidic	HCl	1	0.5
2	Acidic	H_2SO_4	0.3	0.5
3	Neutral	NaCl	6.9	0.6
4	Alkaline	NaOH	8.6	0.5

Table 5. L9 with input and response parameters.

Ex.No	Melting temperature ºC	Stirring speed rpm	Stirring duration minutes	wt.% of B$_4$C and ZrO$_2$	Vickers hardness
1	700	200	10	6	101
2	700	250	15	8	107
3	700	300	20	10	103
4	750	200	15	10	103
5	750	250	20	6	104
6	750	300	10	8	116
7	800	200	20	8	102
8	800	250	10	10	104
9	800	300	15	6	105

Table 6. Response Table for Means of Vickers micro hardness.

Level	Melting temperature ºC	Stirring speed rpm	Stirring duration minutes	wt.% of B4C and ZrO$_2$
1	104.2	102.2	**107.2**	103.5
2	**107.7**	105.0	105.0	**108.3**
3	103.7	**108.3**	103.3	103.7
Delta	**4.0**	**6.2**	**3.8**	**4.8**
Rank	3	1	4	2

Experimental Investigation on Corrosion Behavior of Ultrasonic Assisted stir Cast AA6061 Hybrid Metal
Matrix Composite under DifferentAqueous Corrosive Environments

7

performed and the average value has been taken and it is 116 HV.

3.2. Selection of better combination of optimized ultrasonic stir casted AA6061 HMMC based on micro hardness

The results of Vickers hardness for AA6061/B_4C/ZrO_2 HMMCs are displayed in Table 7 and Figure 5. From the obtained hardness tests, it is observed that the hardness of AA6061 HMMCs is enhanced up to addition of 8wt.% of B_4C and ZrO_2 and decreased the hardness while adding 10wt.% of B4C and ZrO_2. At lower to moderate levels of reinforcement (up to 8 wt.%), the hard particles of B_4C and ZrO_2 are well-distributed within the AA6061 matrix. These particles act as barriers to dislocation movement, enhancing the overall strength and hardness of materials. At 8 wt. %, the distribution of the ceramic particles within the matrix is typically optimal. This creates a well-balanced composite where the hard reinforcements are effectively dispersed without significant agglomeration, leading to maximum enhancement in hardness[34]. The increased hardness of the HMMC is attributed to the inherent hardness of zirconium dioxide and boron carbide ceramic particles, as well as their ability to provide dispersion strengthening and establish strong interparticle bonds within the composite. These ceramic particles, ZrO_2 and B_4C, act as dispersion hardening agents in the matrix, thereby enhancing matrix hardness and contributing to grain size reduction and matrix strengthening.

Table 7. Vickers hardness of AA6061 HMMCs.

S.No	Material composition in wt.%	Vickers hardness
1	AA6061	75
2	AA6061/2wt.%B_4C/2wt.%ZrO_2	86.2
3	AA6061/4wt.%B_4C/4wt.%ZrO_2	94
4	AA6061/6wt.%B_4C/6wt.%ZrO_2	105
5	AA6061/8wt.%B_4C/8wt.%ZrO_2	116
6	AA6061/10wt.%B_4C/10wt.%ZrO_2	109

As the weight percentage of reinforcements increases to 10 wt.%, B_4C and ZrO_2 particles are more likely to agglomerate. This clustering reduces the effective load transfer between the matrix and the reinforcement particles, leading to weak points within the composite structure. At higher concentrations, the interface between the aluminum matrix and the ceramic particles may become less cohesive. This can introduce microvoids or weak bonding regions that compromise the ability of composite to effectively transfer and withstand mechanical loads. Hence, the AA6061/8wt.%B_4C/8wt.%ZrO_2 HMMC is selected for this further investigation[35].

3.3. Metallurgical examination

The ultrasonic stir-cast AA6061/ZrO_2/B_4C HMMC was subjected to XRD and SEM testing to determine the weight percentage of the matrix and reinforcements, and to confirm the uniform dispersion of the reinforcements in the matrix material.

The XRD results and SEM images of AA6061/8 wt.% ZrO_2/8 wt.% B_4C HMMC are displayed in Figure 6a and 6b. The high peaks of ZrO_2, B_4C, and Al are observed at 71.4, 35.68, and 37.81 degrees 2 theta values, respectively[36]. The SEM image of the ultrasonic-aided stir-cast AA6061-based composite confirms the uniform distribution of zirconium dioxide and boron carbide reinforcements. Additionally, there is no oxide formation on the surface of the stir-cast AA6061 composites due to the casting process being conducted in an inert environment. The cast AA6061/8 wt.% ZrO_2/8 wt.% B_4C composite surface exhibits no porosity due to the use of an ultrasonic vibrator, which prevents the formation of holes caused by the escape of unwanted gases[7].

3.4. Density of AA6061 HMMC composite

The experimental density of the ultrasonic stir-cast AA6061/8 wt.% ZrO_2/8 wt.% B_4C was determined using the Archimedes principle. The measured experimental density of the AA6061-based composite is 2.7652 g/cm³, while the density of the matrix AA6061 is 2.71 g/cm³. The density of zirconium dioxide and boron carbide is higher than that of the AA6061 matrix material; thus, adding both zirconium dioxide and boron carbide reinforcements increases the density of the AA6061/8 wt.% ZrO_2/8 wt.% B_4C HMMC
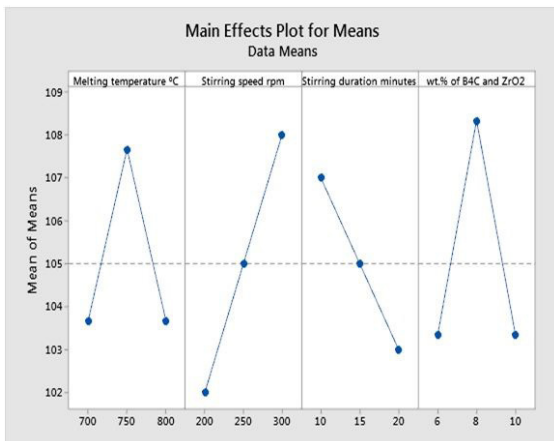

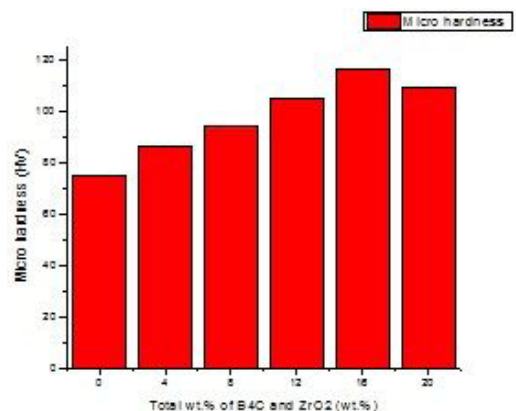**Figure 4.** Main effect plot for Vickers hardness.
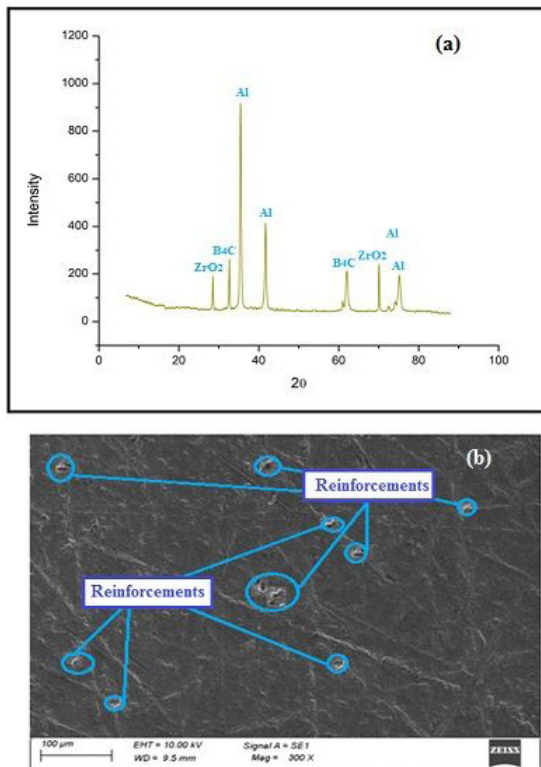

Figure 5. Comparison of micro hardness.

Figure 6. (a)XRD of AA6061/8wt.%ZrO$_2$/8wt.%B$_4$C; (b) SEM image of AA6061/8wt.%ZrO$_2$/8wt.%B$_4$C.

Figure 7. Comparison of AVG.OCP of AA6061 composite with various electrolytes.

composite. The removal of porosity is achieved through the use of an ultrasonic vibrator, which ensures the even distribution of both zirconium dioxide and boron carbide throughout the AA6061 matrix material. Ultrasonic vibration sends high-frequency sound waves into the material, causing fast oscillations. These oscillations cause molten metal to form cavitation bubbles. When these bubbles collapse, they release considerable energy and pressure, dispersing the ZrO$_2$ and B$_4$C particles evenly throughout the AA6061 matrix. This equal distribution reduces the danger of particle agglomeration, a typical source of porosity in composite materials. Ultrasonic vibrations dynamically mix ZrO$_2$ and B$_4$C particles, ensuring equal distribution and suspension throughout the matrix during solidification. This prevents particles from settling or collecting in specific places, which can generate localised zones of weakness or porosity. Moreover, ultrasonic vibrations provide dynamic mixing of ZrO$_2$ and B$_4$C particles, ensuring their even distribution and suspension within the matrix during the solidification process. This action prevents the particles from settling or clustering in specific areas, thereby avoiding localized zones of weakness or porosity[37].

3.5. Assessment of OCP

The Open Circuit Potential (OCP) is a useful metric for determining the corrosion resistance of an AA6061/8wt.% ZrO$_2$/8 wt.% B$_4$C working electrode. This measurement provides i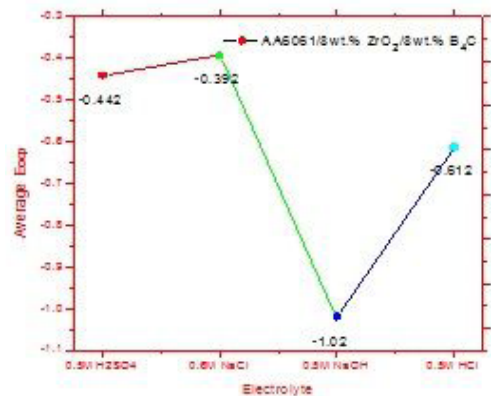nformation about the intrinsic or equilibrium potential of the AA6061/8wt.% ZrO$_2$/8 wt.% B$_4$C working electrode in a given environment, allowing for the prediction of its corrosion response. Separate electrochemical cells should be set up for each of the four environments (H$_2$SO$_4$, NaOH, NaCl, and HCl). Each cell should contain the AA6061/8 wt.% ZrO$_2$/8 wt.% B$_4$C composite electrode, a platinum electrode, and an Ag/AgCl reference electrode. When the electrochemical cells are first set up, measure the OCP values for the composite electrode in each of the four environments.

These initial OCP measurements will serve as a baseline for analyzing corrosion behavior. Monitor the OCP values in each cell at 1-hour intervals. The results from the OCP measurements and the average OCP value are displayed in Figure 7. A multitude of variables can impact the electrochemical behavior of a composite electrode like AA6061/8wt.% ZrO$_2$/8 wt.% B$_4$C in different electrolytes (NaCl, H$_2$SO$_4$, NaOH, and HCl), including the electrode material, the nature of the electrolyte, and the redox processes occurring in the system. The AA6061/8wt.%ZrO$_2$/8 wt.% B$_4$C composite electrode is composed of aluminum (AA6061), zirconia (ZrO$_2$), and boron carbide (B$_4$C). These materials exhibit various electrochemical characteristics, including reactivity, conductivity, and catalytic activity, which can influence the electrochemical behavior of the electrode in different electrolytes. The choice of electrolyte (NaCl, H$_2$SO$_4$, NaOH, or HCl) is critical because it affects the ions and chemical reactions occurring at the electrode-electrolyte interface. Each electrolyte has different ionic species that significantly influence electrode behavior.

The electrochemical potential difference between the composite electrode and the reference electrodes (Platinum and Ag/AgCl) is determined by the redox processes occurring at the electrode/electrolyte interface. The presence of chloride ions (Cl-) in NaCl, for example, might induce redox reactions that impact the electrode potential. Specific ions in the electrolyte can absorb onto the electrode surface and alter its electrochemical characteristics[38]. For instance, in NaCl, chloride ions may interact differently with the electrode compared to ions present in other electrolytes, resulting in varied potentials. The higher positive cathodic potential

Experimental Investigation on Corrosion Behavior of Ultrasonic Assisted stir Cast AA6061 Hybrid Metal
Matrix Composite under DifferentAqueous Corrosive Environments

9

observed in the NaCl electrolyte for the AA6061/8 wt.% ZrO_2/8 wt.% B_4C composite electrode, compared to H_2SO_4, NaOH, and HCl, is likely due to a combination of factors, including the specific chemistry of the electrolyte, the properties of the electrode material, the pH, and the effects of specific ions. The higher cathodic potential is achieved in the following sequence of electrolytes: NaCl, H_2SO_4, NaOH, and HCl.

3.6. Potentiodynamic polarization characterisation

Potentiodynamic polarization is a common electrochemical method used to investigate the corrosion behavior of AA6061/8 wt.% ZrO_2/8 wt.% B_4C composite materials. It involves monitoring the current response of a metal electrode while varying its potential in an electrochemical cell containing electrolytes such as NaCl, H_2SO_4, NaOH, and HCl. The resulting graph is called a potentiodynamic polarization curve, which provides crucial information about the corrosion properties of materials. Interpreting the potentiodynamic polarization plot can reveal information about a corrosion resistance of material and its susceptibility to localized corrosion, such as pitting or crevice corrosion.

The corrosion potential (Ecorr) is the potential at which the anodic and cathodic currents balance. The corrosion current density (Icorr) is related to the corrosion rate. The anodic curve shows a passivation area with low current density, indicating the presence of a passive oxide layer. The critical pitting potential (Ecp) and critical passivation potential (Ecpp)

are the potentials at which pitting corrosion or repassivation can occur. The PDP plot for the AA6061/8 wt.% ZrO_2/8 wt.% B_4C working electrode is displayed in Figure 8. Lower current density and potential indicate higher corrosion resistance. Higher corrosion resistance is observed for the AA6061/8 wt.% ZrO_2/8 wt.% B_4C working electrode in a 0.6 M NaCl electrolyte solution concerning current potential. Similarly, higher corrosion resistance is observed for the AA6061/8 wt.% ZrO_2/8 wt.% B_4C working electrode in a 0.5 M NaOH electrolyte solution concerning current density.

Chloride ions are well-known for their capacity to promote corrosion, particularly pitting corrosion, in several metals, including aluminum (AA6061). When the AA6061/8 wt.% ZrO_2/8 wt.% B_4C working electrode is tested in a chloride-rich environment such as 0.6 M NaCl, significant corrosion susceptibility is expected[39]. If this electrode demonstrates superior corrosion resistance compared to other electrodes in NaCl, it suggests that the additions of ZrO_2 and B_4C have a passivating effect, forming a protective coating on the surface that mitigates chloride-induced corrosion. An example of an alkaline solution is 0.5 M NaOH. Aluminium and aluminium alloys exhibit greater corrosion resistance in alkaline conditions than in acidic ones. The alkaline environment can prompt the surface to form a protective coating of aluminum oxide (Al_2O_3), which acts as a barrier against further corrosion. The incorporation of ZrO_2 and B_4C additives may further enhance this passivation effect. Acidic solutions, such as H_2SO_4 and HCl, are known examples. Aluminum is particularly susceptible to corrosion in acidic conditions because protons (H+) can accelerate its
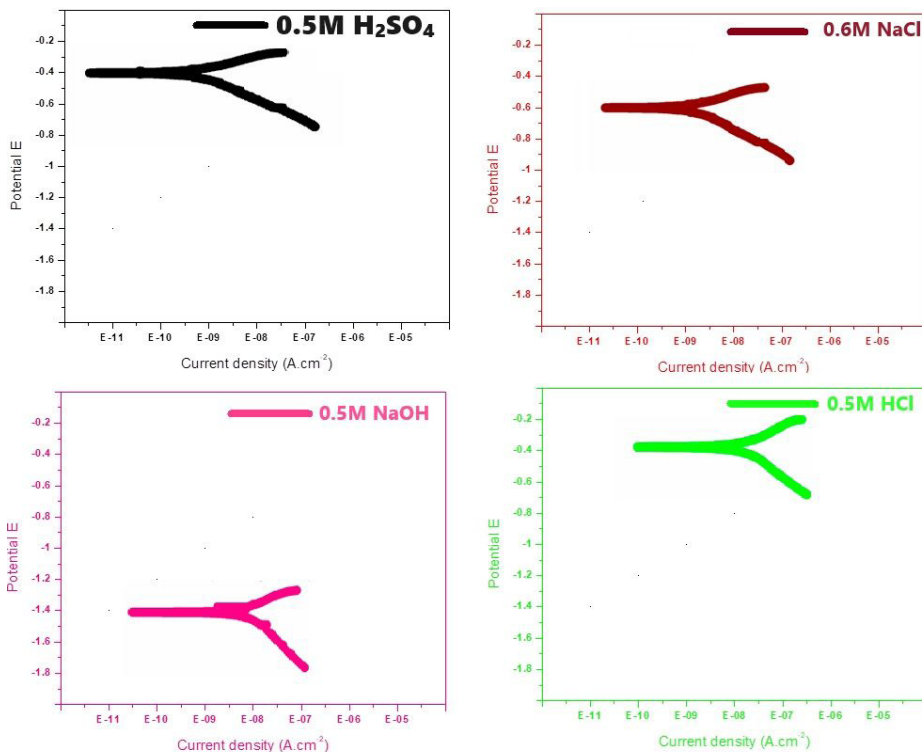

Figure 8. PDP plots for different electrolytes.

degradation. Additionally, the presence of chloride ions in HCl can be highly corrosive. Due to the lower concentration of chloride ions, the 0.6 M NaCl solution may be less aggressive than HCl.

3.7. Electrochemical impedance spectroscopy (EIS)

EIS evaluates the impedance of an electrochemical system across a wide frequency range. Impedance is a multidimensional quantity that includes both resistance (the real portion) and reactance (the imaginary part). EIS involves applying a low-amplitude alternating current voltage to the working electrode and monitoring the resulting current response. The system impedance is then determined as the ratio of the applied voltage to the measured current. By analyzing the impedance data, particularly the polarisation resistance (Rp) obtained from the equivalent circuit model, EIS can be used to predict the corrosion rate. The Tafel equation, which defines the relationship between the corrosion current density (i_corr) and Rp, connects polarisation resistance to the corrosion rate. Faraday's law is then used to calculate the corrosion rate (CR). The corrosion rate can be calculated both with and without a protective film or coating. The difference in corrosion rates between the two conditions provides information about the effectiveness of the preventive measures. Localized corrosion processes, such as pitting corrosion, can also be detected and characterized using EIS. Changes in impedance and the appearance of specific impedance characteristics can indicate the initiation and spread of localized corrosion. The electrochemical kinetics of corrosion processes, the presence and characteristics of passive films, and the effects of inhibitors and coatings on corrosion behavior can all be assessed using EIS. The EIS measurement and Bode plot for AA6061//8 wt.% ZrO_2/8 wt.% B_4C in various corrosive environments such as NaOH, HCl, H_2SO_4, and NaCl are displayed in Table 8 and Figure 9. Rs, which stands for "Solution Resistance," indicates the resistance associated with the bulk of the solution through which the electrical current flows. It is measured in ohms per square centimeter ($\Omega\cdot cm^2$). Lower Rs values often imply stronger electrical conductivity of the solution. Rct, or "Charge Transfer Resistance," represents the resistance associated with the electrochemical processes occurring at the interface between the material under study and the corrosive solution. It can alternatively be expressed in ohms per square centimeter ($\Omega\cdot cm^2$). A higher Rct number suggests that the material will corrode more slowly or will be more resistant to corrosion. CPE1 is an abbreviation for "Constant Phase Element 1." This component is used in the electrochemical system modeling of non-ideal capacitive behavior. This characteristic indicates capacitance and is related to the Constant Phase Element 1 (CPE1). The units of measurement are Farads per square centimeter (F/cm^2).

Capacitance measures a capacity of materials to hold electrical charge. CPE1 and n1 are parameters linked to Constant Phase Element 1, used to describe non-ideal capacitive behavior or the exponent in a mathematical model. This characteristic, like CPE1 P1, may be connected to another capacitance (P2) in the system and is measured in farads per square centimeter (F/cm^2). Another parameter, CPE2 and n2, is likely related to the second capacitance (CPE2 P2) and its non-ideal behavior. Higher Rct values often indicate stronger corrosion resistance. CPE parameters simulate non-ideal capacitive behavior in an electrochemical system. The AA6061/8 wt.% ZrO_2/8 wt.% B_4C composite electrode achieves higher Rct values in NaCl corrosive environments, indicating greater corrosion resistance.

CPE1 and CPE2 represent the capacitance between the electrolyte and HMMCs, and between the HMMC and oxide layers, respectively. The CPE1 value for NaCl is higher than that for NaOH, indicating higher resistance. Conversely, the CPE2 value for NaOH is higher than that for NaCl, which signifies higher corrosion resistance by reducing the formation of more elements during the corrosion test. The higher Rct value, lower Rs value, higher CPE1 value, and lower CPE2 value of the AA6061/8 wt.% ZrO_2/8 wt.% B_4C working electrode indicate greater resistance in a NaCl environment[40].

A high Rct indicates strong resistance to charge transfer, suggesting a surface that is more passive and resistant to corrosion. A low Rct indicates easier charge transfer, often due to active corrosion processes occurring on the surface. The aluminum matrix in AA6061/B_4C/ZrO_2 composites is susceptible to corrosion. The presence of B_4C and ZrO_2 can modify the local electrochemical environment, influencing charge transfer kinetics at the interface with the aluminum matrix. B_4C and ZrO_2 can alter surface properties, potentially
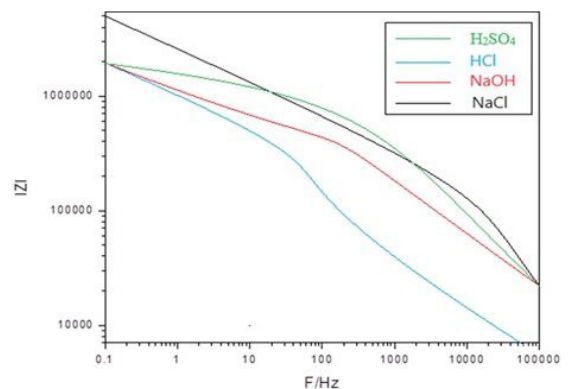

Figure 9. EIS Bode plots.

Table 8. Measurement of EIS.

Corrosion agent	Rs, $\Omega.cm^2$	Rct, $\Omega.cm^2$	CPE_1		CPE_2		W ($\Omega.cm^2$)
			P1 (F/cm^2)	n_1	P2 (F/cm^2)	n_2	
NaCl	2.0152	2.8975×10^5	5.437×10^{-9}	0.624	1.954×10^{-7}	0.362	9.95×10^6
NaOH	0.5216	3.6247×10^5	1.321×10^{-9}	0.665	8.436×10^{-7}	0.453	1.32×10^6
HCl	1.9021	2.1235×10^5	2.362×10^{-9}	0.681	2.701×10^{-7}	0.453	7.01×10^6
H_2SO_4	1.9652	2.9634×10^5	1.954×10^{-9}	0.653	2.465×10^{-7}	0.392	3.92×10^6

Experimental Investigation on Corrosion Behavior of Ultrasonic Assisted stir Cast AA6061 Hybrid Metal
Matrix Composite under DifferentAqueous Corrosive Environments

11

impacting the formation of corrosion-resistant layers or barriers. The interaction between these particles and the aluminum matrix can change charge transfer processes, thereby affecting Rct.

The Bode plot is an effective tool for evaluating the corrosion behavior of AA6061/8 wt.% ZrO_2/8 wt.% B_4C working electrode materials in various conditions, such as NaCl, NaOH, H_2SO_4, and HCl. The AA6061/8 wt.% ZrO_2/8 wt.% B_4C working electrode exhibits higher corrosion resistance in a NaCl environment due to the higher |Z| value compared to other environments. Figure 9 demonstrates that the composite electrode has the highest corrosion resistance in a NaCl environment, followed by H_2SO_4, NaOH, and HCl environments. Aluminium and its alloys are more corrosion resistant in alkaline than acidic environments because the mild alkaline environment promotes the creation and maintenance of a protective oxide layer. This coating considerably reduces additional rusting. In contrast, acidic circumstances cause the protective coating to dissolve quickly, exposing the aluminium to accelerated corrosion. In slightly alkaline conditions (pH 7-10), aluminium forms a protective layer of aluminium hydroxide $(Al(OH)_3)$ and/ or oxide (Al_2O_3).This protective coating is highly insoluble and sticky, functioning as a barrier to greatly inhibit the corrosion process by preventing the underlying metal from interacting with the environment. In acidic settings (pH < 7), especially at low pH values, the protective aluminium oxide layer might disintegrate, leaving the metal vulnerable to the aggressive action of hydrogen ions (H^+). The breakdown of the oxide layer hastens the corrosion process by leaving the aluminium surface vulnerable[40].

The inclusion of B_4C and ZrO_2 within the AA6061 composite can establish galvanic interactions with the aluminum matrix. Depending on the pH levels and ion concentration in the environment, aluminum may undergo preferential corrosion, which could lead to faster degradation in certain conditions. Both the pH and the presence of specific ions influence the formation and stability of protective layers on the surface of the composites. For instance, ions can facilitate the development of a durable oxide or hydroxide film that shields the composite from further corrosion. The junction between the aluminum matrix and the reinforcing particles (B_4C/ZrO_2) is often susceptible to localized corrosion, especially in harsh environments characterized by low pH and high chloride ion content[41,42].

3.8. Metallurgical examination of corroded surfaces

The morphology of the corroded surface of AA6061/8 wt.% ZrO_2/8 wt.% B_4C HMMC under NaCl, NaOH, HCl, and H_2SO_4 conditions is analyzed using SEM. The presence of elements in the corroded surfaces is also analyzed using EDS.

Figure 10 displays the morphology of corroded AA6061/8 wt.% ZrO_2/8 wt.% B_4C HMMC under different
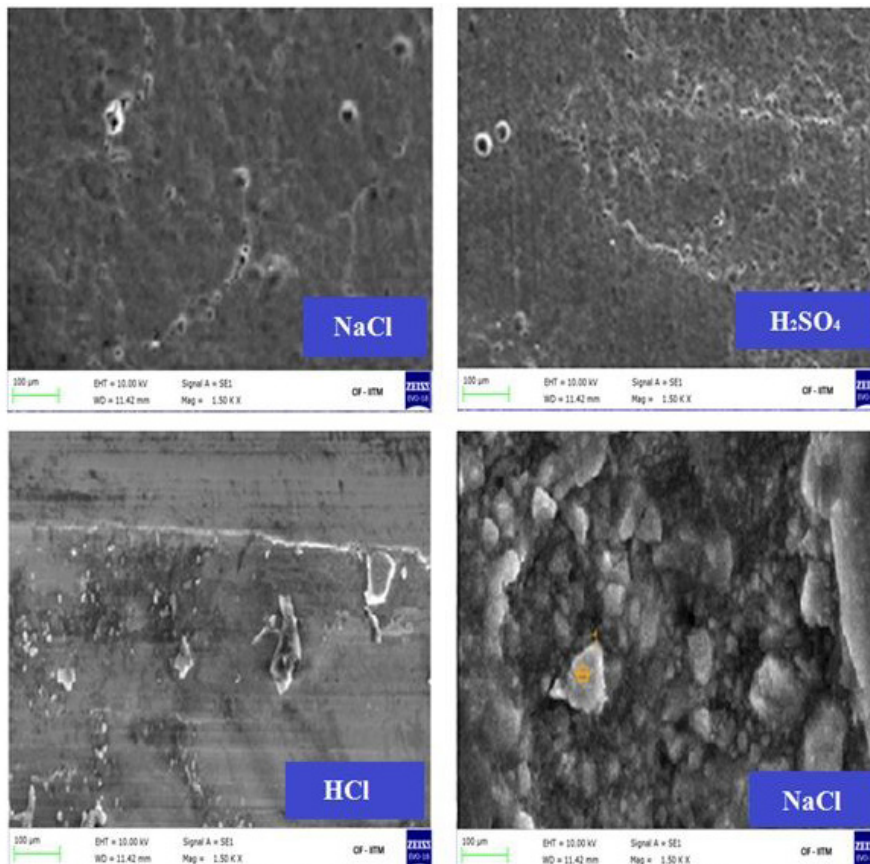

Figure 10. Morphology of corroded surface of AA6061 HMMC with 100 µm under different corrosive environments.
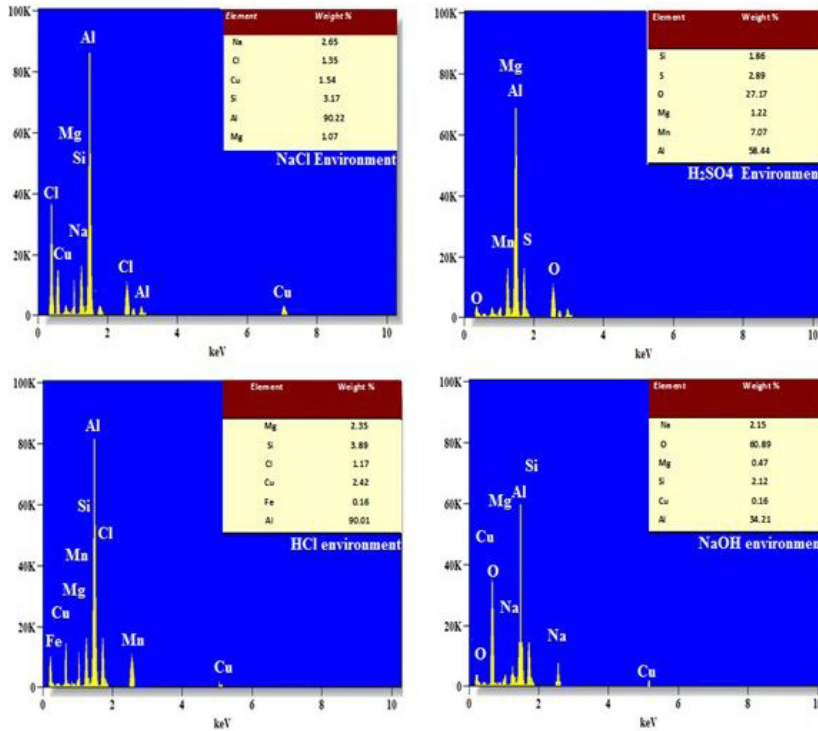
Figure 11. EDS result of corroded surface of AA6061 HMMC under different corrosive environments.

corrosive environments. Figure 11 shows the EDS results of corroded AA6061/8 wt.% ZrO_2/8 wt.% B_4C HMMC under these environments. Na and Cl are deposited on the surface of the corroded AA6061-based HMMC under NaCl conditions. S and O are found on the surface of the corroded AA6061-based HMMC under H_2SO_4 conditions. Cl is deposited on the corroded surface of the AA6061-based HMMC under HCl conditions. Na and O are deposited on the surface of the corroded AA6061-based HMMC under NaOH conditions. The surfaces exposed to NaOH, HCl, and H_2SO_4 show more severe corrosion compared to the surface exposed to NaCl. The AA6061 HMMC experiences less corrosion when exposed to NaCl. The surfaces exposed to NaOH, HCl, and H_2SO_4 show more severe corrosion compared to the surface exposed to NaCl. The AA6061 HMMC experiences less corrosion when exposed to NaCl[43-45].

4. Conclusions

The AA6061/8wt.% ZrO_2/8wt.% B_4C HMMC was fabricated using an ultrasonic-assisted stir casting setup. The XRD test on the fabricated AA6061 HMMC confirmed the presence of the added weight percentages of Al, ZrO_2, and B_4C. The uniform distribution of reinforcements and the removal of porosity were confirmed by the SEM test on the AA6061 HMMC. The determined experimental density and microhardness of the AA6061-based composite are 2.7652 g/cm^3 and 116 HV, respectively. The higher corrosion resistance of the AA6061 HMMC was confirmed under NaCl environment through PDP plots, Bode plots, and assessment of OCP. The formation of Cl-ions offered resistance to

corrosion. The morphology of the corroded surface of the AA6061 HMMC under the NaOH environment was highly affected by the corrosion mechanism, as confirmed by the SEM test. The high amount of Cl deposition on the surface of the corroded AA6061 HMMC under the NaCl environment led to the formation of an oxide protective layer, resisting corrosion, as confirmed by the EDS test.

5. References

1. Mohajerani A, Burnett L, Smith JV, Kurmus H, Milas J, Arulrajah A, et al. Nanoparticles in construction materials and other applications, and implications of nanoparticle use. Materials. 2019;12(19):3052.
2. Vieyra H, Molina-Romero JM, Calderón-Nájera JD, Santana-Díaz A. Engineering, recyclable, and biodegradable plastics in the automotive industry: a review. Polymers. 2022;14(16):3412. http://doi.org/10.3390/polym14163412.
3. Yang S. Properties, applications, and prospects of carbon nanotubes in the construction industry. Archit Struct Constr. 2023;3(3):289-98.
4. Nturanabo F, Masu L, Baptist Kirabira J. Novel applications of aluminium metal matrix composites. London: IntechOpen; 2020.
5. Ujah CO, Kallon DVV. Trends in aluminium matrix composite development. Crystals. 2022;12(10):1357.
6. Ashebir DA, Mengesha GA, Sinha DK. An insight into mechanical and metallurgical behavior of hybrid reinforced aluminum metal matrix composite. Adv Mater Sci Eng. 2022;e843981.
7. Kareem A, Qudeiri JA, Abdudeen A, Ahammed T, Ziout A. A review on AA 6061 metal matrix composites produced by stir casting. Materials. 2021;14(1):175.
8. Parveez B, Kittur MI, Badruddin IA, Kamangar S, Hussien M, Umarfarooq MA. Scientific advancements in composite materials for aircraft applications: a review. Polymers. 2022;14(22):5007.

Experimental Investigation on Corrosion Behavior of Ultrasonic Assisted stir Cast AA6061 Hybrid Metal
Matrix Composite under DifferentAqueous Corrosive Environments

13

9. Vani VV, Chak SK. The effect of process parameters in aluminum metal matrix composites with powder metallurgy. Manuf Rev. 2018;5:7.

10. Manghnani S, Shekhawat D, Goswami C, Patnaik TK, Singh T. Mechanical and tribological characteristics of Si_3N_4 reinforced aluminium matrix composites: a short review. Mater Today Proc. 2021;44(Part 6):4059-64.

11. Singh H, Singh K, Vardhan S, Mohan S. Comprehensive review on the new developments consideration in a stir casting processing of aluminum matrix composites. Mater Today Proc. 2022;60(Part 2):974-81.

12. Pandiyarajan R, Maran P, Marimuthu S, Arumugam K. Mechanical and metallurgical characterization of friction stir welded AA6061- ZrO2-C hybrid MMCs. Mater Today Proc. 2019;19(Part 2):256-9.

13. Pradhan SK, Chatterjee S, Mallick AB, Das D. A simple stir casting technique for the preparation of in situ Fe-aluminides reinforced Al-matrix composites. Perspect Sci. 2016;8:529-32. http://doi.org/10.1016/j.pisc.2016.06.011.

14. Cao H, Luo Z, Wang C, Wang J, Hu T, Xiao L, et al. The stress concentration mechanism of pores affecting the tensile properties in vacuum die casting metals. Materials. 2020;13(13):3019.

15. Sambathkumar M, Gukendran R, Mohanraj T, Karupannasamy DK, Natarajan N, Christopher DS. A systematic review on the mechanical, tribological, and corrosion properties of al 7075 metal matrix composites fabricated through stir casting process". Adv Mater Sci Eng. 2023;2023:1-17.

16. Chebolu R, Nallu R, Chanamala R, Sharma SK, Rudrapati R. Influence of SiC/TiB_2 particles addition on corrosion behavior of As-Cast Zn-Al-Cu alloy hybrid composites. J Eng. 2022: 1-5.

17. Tirlangi S, Rao PS. Microstructure and corrosion investigation of A356 varying reinforced with graphite and granite composites. Int J Mech Prod Eng Res Dev. 2019;9(6):191-200.

18. Govindan K, Raghuvaran JGT. Mechanical properties and metallurgical characterization of $LM25/ZrO_2$ composites fabricated by stir casting method. Materia. 2019;24(3):e12439.

19. Arab M, Azadi M, Mirzaee O. Effects of manufacturing parameters on the corrosion behavior of Al–B_4C nanocomposites. Mater Chem Phys. 2020;253:123259.

20. Yunus M, Alfattani R. Assessment of mechanical and tribological behavior of AA6061 reinforced with B_4C and Gr hybrid metal matrix composites. Coatings. 2023;13(9):1653.

21. Kamaraj L, Sudhan HS, Moshi AM. Optimizing the ultrasonication effect in stir-casting process of aluminum hybrid composite using desirability function approach and artificial neural network. J Mater Des Applic. 2021;235(9):2007-21.

22. Kumar D, Thakur L. A study of processing and parametric optimization of wear-resistant AZ91-TiB_2 composite fabricated by ultrasonic-assisted stir casting process. Surf Topogr. 2022;10(2):025024.

23. Kumar SD, Ravichandran M, Jeevika A, Stalin B, Kailasanathan C, Karthick A. Effect of ZrB2 on microstructural, mechanical and corrosion behaviour of aluminium (AA7178) alloy matrix composite prepared by the stir casting route. Ceram Int. 2021;47(9):12951-62.

24. Deng SH, Lu H, Li D. Effect of UV light illumination on the corrosion behavior of electrodeposited TiO_2 -Ni composite foils. Appl Surf Sci. 2018;462:291-302.

25. Singh H, Singh K, Vardhan S, Mohan S. Study on the wear performance of AA 6061 and AA 6082 based metal matrix composites. Mater Today Proc. 2021;43(Part 1):660-4.

26. Kumar BA, Krishnan MM, Sahayaraj AF, Refaai MRA, Yuvaraj G, Madhesh D, et al. Characterization of the aluminium matrix composite reinforced with silicon nitride ($AA6061/Si_3N_4$) synthesized by the stir casting route. Adv Mater Sci Eng. 2022 : 2 : 1-8

27. Balamurugan K, Shanmugam V, Palani G, Sundarakannan R, Sathish T, Linul E, et al. Effect of TiC/RHA on solid particle erosion of Al6061 hybrid composites fabricated through a 2-step ultrasonic-assisted stir casting process. J Mater Res Technol. 2023;25:4888.

28. Muniappan A, Thiagarajan C, Senthiil PV, Jayakumar V, Shaafi T. Effect of wire-EDM process parameters on cutting speed of AL6061 hybrid composite. Int J Mech Eng Technol. 2017;8(10):185-9.

29. Mohanty P, Mahapatra R, Padhi P, Ramana C, Mishra DK. Ultrasonic cavitation: an approach to synthesize uniformly dispersed metal matrix nanocomposites: a review. Nano-Struct Nano-Objects. 2020;23:100475.

30. Vincent B, Ramesh B. Comparison of ASTM plastic and composite standards on mechanical properties of GFRP composites. Int J Appl Eng Res. 2015;10(68):686-8.

31. Rosliza R, Senin HB, Nik WBW. Electrochemical properties and corrosion inhibition of AA6061 in tropical seawater. Colloids Surf A Physicochem Eng Asp. 2008;312(2-3):185-9.

32. Chen J, Xu W, Wang X, Yang S, Xiong C. Progress and applications of seawater activated batteries. Sustainability. 2023;15(2):1635.

33. Senthil Kumar S, Senthilkumar TS, Pitchipoo P, Dwivedi YD, Nagaprasad N, Saxena KK, et al. Grey relational analysis and surface texture analysis of Al-based metal matrix composites. J Mater Res Technol. 2023;24:5372-88.

34. Khan AH, Shah SAA, Umar F, Noor U, Gul RM, Giasin K, et al. Investigating the microstructural and mechanical properties of novel ternary reinforced AA7075 hybrid metal matrix composite. Materials. 2022;15(15):5303.

35. Varol T, Canakci A. Effect of particle size and ratio of B_4C reinforcement on properties and morphology of nanocrystalline Al2024-B_4C composite powders. Powder Technol. 2013;246:462.

36. Gergely A. A review on corrosion protection with single-layer, multilayer, and composites of graphene. Corros Rev. 2018;36(2):155-225.

37. Khavari M, Priyadarshi A, Morton J, Porfyrakis K, Pericleous K, Eskin D, et al. Cavitation-induced shock wave behaviour in different liquids. Ultrason Sonochem. 2023;94:106328.

38. Wei W, Xu J, Chen W, Mi L, Zhang J. A review of sodium chloride-based electrolytes and materials for electrochemical energy technology. J Mater Chem A Mater Energy Sustain. 2022;10(6):2637.

39. Souza LM, Pereira E, Amaral TBS, Monteiro SN, Azevedo ARG. Corrosion study on duplex stainless steel UNS S31803 subjected to solutions containing chloride ions. Materials. 2024;17(9):1974.

40. Qin P, Chen LY, Liu YJ, Zhao CH, Lu YJ, Sun H, et al. Corrosion behavior and mechanism of laser powder bed fusion produced CoCrW in an acidic NaCl solution. Corros Sci. 2023;213:110999.

41. Lee J, Srimuk P, Fleischmann S, Su X, Hatton TA, Presser V. Redox-electrolytes for non-flow electrochemical energy storage: a critical review and best practice. Prog Mater Sci. 2019;101:46-89.

42. Mindivan H. A study on the corrosion and tribocorrosion behavior of Al-30 Vol.% B_4C composite produced by mechanical milling and hot pressing. J Mater Eng Perform. 2021;30(12):9140.

43. Han YM, Chen XG. Electrochemical behavior of Al-B_4C metal matrix composites in NaCl solution. Materials. 2015;8(9):6455-70.

44. Swamy PK, Mylaraiah S, Chandrashekarappa MPG, Lakshmikanthan A, Pimenov DY, Giasin K, et al. Corrosion behaviour of high-strength Al 7005 alloy and its composites reinforced with industrial waste-based fly ash and glass fibre: comparison of stir cast and extrusion conditions. Materials. 2021;14(14):3929.

45. Wicaksono AB, Sutanto H, Ruslan W. Effects of immersion in the NaCl and H_2SO_4 solutions on the corrosion rate, microstructure, and hardness of stainless steel 316L. Res Eng Struct Mater. 2023;9(4):1153-68.